

Radiative recombination in $\text{In}_{0.15}\text{Ga}_{0.85}\text{N}/\text{GaN}$ multiple quantum well structures

B. Monemar¹, J. P. Bergman¹, J. Dalfors¹, G. Pozina¹, B.E. Sernelius¹, P.O. Holtz¹, H. Amano^{2,3} and I. Akasaki^{2,3}

¹*Department of Physics and Measurement Technology, Linköping University,*

²*Department of Electrical and Electronic Engineering, Meijo University,*

³*High-Tech Research Center, Meijo University,*

(Received Thursday, September 9, 1999; accepted Saturday, December 4, 1999)

We present a study of the radiative recombination in $\text{In}_{0.15}\text{Ga}_{0.85}\text{N}/\text{GaN}$ multiple quantum well samples, where the conditions of growth of the InGaN quantum layers were varied in terms of growth temperature (< 800 °C) and donor doping. The photoluminescence peak position varies strongly (over a range as large as 0.3 eV) with delay time after pulsed excitation, but also with donor doping and with excitation intensity. The peak position is mainly determined by the Stark effect induced by the piezoelectric field. In addition potential fluctuations, originating from segregation effects in the InGaN material, from interface roughness, and the strain fluctuations related to these phenomena, play an important role, and largely determine the width of the emission. These potential fluctuations may be as large as 0.2 eV in the present samples, and appear to be important for all studied growth temperatures for the InGaN layers. Screening effects from donor electrons and excited electron-hole pairs are important, and account for a large part of the spectral shift with donor doping (an upward shift of the photoluminescence peak up to 0.2 eV is observed for a Si donor density of $2 \times 10^{18} \text{ cm}^{-3}$ in the well), with excitation intensity and with delay time after pulsed excitation (also shifts up to 0.2 eV). We suggest a two-dimensional model for electron- and donor screening in this case, which is in reasonable agreement with the observed data, if rather strong localization potentials of short range (of the order 100 Å) are present. The possibility that excitons as well as shallow donors are impact ionized by electrons in the rather strong lateral potential fluctuations present at this In composition is discussed.

1 Introduction

$\text{In}_x\text{Ga}_{1-x}\text{N}/\text{GaN}$ multiple quantum well (MQW) structures provide an important active medium for the violet III-Nitride lasers [1]. The recombination processes in these structures therefore are of considerable interest. It has recently been claimed that the broad spontaneous photoluminescence (PL) emission spectra in these structures are due to an inhomogeneously broadened envelope of excitonic emissions from "quantum dots" (QDs) [2] [3]. These QDs are supposed to consist of regions of a size 3-5 nm having a bandgap much lower than the alloy matrix, due to segregation of In during growth [2]. Other recent work points towards the importance of the piezoelectric field as the dominant mechanism governing the electronic energy levels and the recombination processes in these QW structures [4] [5]. In the previ-

ous studies the In composition x in the QWs was typically smaller than $x = 0.15$, and the recombination processes were described in terms of QW excitons [2] [3] [4] [5]. In this work we report on a study of the recombination dynamics in $\text{In}_{0.15}\text{Ga}_{0.85}\text{N}$ MQWs over the temperature range 2 - 300 K. Thin epitaxial layers of InGaN with the same In composition and similar growth conditions as the QW InGaN material have also been studied. By comparing the PL emission properties of samples grown at different (rather low) growth temperatures (< 800 C) for the InGaN layers we conclude that the recombination processes are quite similar in the samples we have studied. The QD exciton model in the specific form of Refs. [2] and [3] is not confirmed in our samples, although clearly carrier localization is important. Multi-peak PL spectra as reported in Ref [2]

are not observed in these samples. The piezoelectric (PZ) field has a strong effect on the recombination, but potential fluctuations are also strong, probably sufficiently strong to destroy excitons in the recombination process, and leading to strong separate carrier localization in most of the temperature range up to 300 K.

2 Samples and experimental procedures

The $\text{In}_x\text{Ga}_{1-x}\text{N}$ MQWs comprising 5 nominally identical QWs were grown with MOCVD with an In fraction x about 0.15 for all samples studied in this work. The QW thickness was 3.0 nm, with a GaN barrier thickness of 6.0 nm, (see a schematic picture in Figure 1). The detailed growth procedures have been described elsewhere [6]. The GaN barriers were grown at high temperatures (about 1000 °C), while the growth temperature of the InGaN layers was lower, and varied between different samples, as specified below. The structural quality was investigated for selected samples. It was found that the interfaces of the QWs were rather smooth, the lower GaN/InGaN interface was virtually atomically flat in high resolution TEM pictures, while the upper InGaN/GaN interface had a short range fluctuation of about 1-2 monolayers. This is presumably due to an instability of the alloy during the growth interruption while increasing the temperature before the next GaN layer was grown. High resolution PL and cathodoluminescence (CL) topographs reveal a difference in spectral homogeneity between samples where the InGaN layers were grown at $T = 700$ °C and $T = 780$ °C, respectively. (Figure 2 (a-c)). In the former case spectral peak wavelength fluctuations (covering a range of < 0.1 eV, and accompanied by intensity fluctuations) occurred on a length scale of a few μm , while in the latter case these fluctuations were of a typical size below 1 μm , but still well resolved. For the case in Figure 2a, b the intensity fluctuations may partly be due to the underlying GaN layer. For Figure 2c the variation on this length scale might be due to an interference of dislocations with the growth habits of the InGaN layers, dependent on the InGaN growth temperature. Since the diffusion length of carriers (or excitons) in the QWs is expected to be well below 100 nm, this large scale variation is not considered to be the only source of spectral broadening, however. Corresponding studies of composition or strain variation in the QWs with atomic resolution (high resolution TEM) were not performed in this work. The expected nano-scale fluctuations of In compositions were therefore not directly documented in these samples, but we will show that there is indirect evidence of their importance. As will be demonstrated below, lowering the growth temperature of the InGaN layers does not seem to decrease the presence of strong localization potentials.

The spectral PL experiments discussed here involve continuous wave (cw) laser excitation, as well as more advanced transient studies. In the former case we have access to two different setups, one with an unconverted cw argon laser (FRED) emitting at 244 nm, together with a 0.32 m monochromator, and a UV-sensitive CCD detector. The other setup employs a tuneable pulsed UV laser. In both cases we use He cryostats for variable temperature experiments from 2 K to 300 K. In the PLE measurements a Xenon lamp together with a double monochromator was used as tuneable excitation source. For the transient PL measurements we had several UV laser systems available, tuneable both above and below the GaN bandgap. For detection we employ photon counting techniques for the time domain 100 ps to 4 μs , and a streak camera for the faster time domain 15 ps to 2 ns.

3 Experimental results

3.1 Photoluminescence spectra for InGaN layers and MQWs. Dependence of growth temperature and donor doping

It is now well established that InGaN has a strong tendency for phase separation when grown at a temperature above about 750 °C [7] [8]. We have studied the influence of this problem on the MQW properties with the aid of four typical nominally undoped samples in this work. Two samples were coherently strained bulk InGaN layers (thickness about 50 nm) grown at different temperatures, 700 °C and 780 °C, respectively. In addition we studied two MQW samples, where the InGaN layers were grown at the same two temperatures. The PL spectra for the coherently strained InGaN layers, grown at 700 °C and 780 °C, respectively, are for both samples composed of a slightly broadened peak with weaker LO phonon replicas towards lower photon energies. (Figure 3). The PL peak energies (with laser excitation) are at 2.81 eV and 2.85 eV, respectively, in fair agreement with other recent data for strained InGaN layers with this composition [4] [9]. The PLE spectra for these emissions are severely broadened (Figure 3c), and no accurate value of a Stokes shift (i.e. difference in peak position in PL emission and PLE) can be obtained. A weak peak at about 2.9 eV may indicate a Stokes shift of about 0.1 – 0.2 eV. This is consistent with the difference between the photoreflectance (PR) data and the PL data in Ref [9]. The large broadening might be an indication of a mixed relaxation regime at this thickness, so that some regions of the layers may be partly relaxed [10]. The transient decay time at 2 K is short, less than 1 ns, in both samples (Figure 4). This is a radiative lifetime, and the value is typical for localized bulk 3D excitons. The localization potentials in this case are the InGaN alloy fluctuations, which are expected to be

amplified by segregation of the alloy. There is evidence of such a process from the weaker low energy peaks present in Figure 3 (b).

In Figure 5 we show the corresponding PL spectra with weak lamp excitation for the two MQW samples, together with PLE spectra. The PL spectra are quite similar for the two samples (apart from a larger width for the lower InGaN growth temperatures), as are the PLE spectra. The PLE curves are more or less featureless ramps, with no sign of excitonic states in the InGaN QW. This is expected from the reduced near bandgap oscillator strength induced by the PZ field, but also from the Stokes shift due to localization potentials. The broad PL peaks are downshifted from the expected position of the unperturbed QW bandgap by about 0.3 - 0.4 eV in both samples. The broad peak also shows a continuous upshift with increased excitation intensity, as shown for one sample in Figure 5c.

We have studied the effect of shallow donor doping in the QW on the optical spectra. A set of samples with the InGaN growth temperature 700 C was Si-doped in the QWs during growth, at doping densities up to $2 \times 10^{18} \text{ cm}^{-3}$. As shown in Figure 6, a strong upshift of the PL peak photon energy is observed with donor doping, which could be expected from screening of both the PZ field and the localization potentials. An observed variation of the peak position across the sample is interpreted as mainly an effect of uneven donor concentration. The effect of donor doping on PL spectra in these samples is surprisingly strong, as discussed in more detail below.

3.2 Transient PL spectra for MQWs

We have investigated the transient behavior of the PL over a wide time scale and dynamic range. On the short time scale there is a very fast capture process into the QW, as evidenced by the very sharp onset of the PL emission across the entire spectrum in the streak camera data (see Figure 7). The rise time is at most corresponding to the time resolution of the set up, i.e. about 15 ps, which is then an upper limit for the rise time of the PL emission. This experiment has been performed with above barrier bandgap excitation as well, leading to a very similar result. The main broad radiative recombination peak is obviously established within a very short time via very fast carrier (or exciton) capture into the QWs. At later times slower processes lead to spectral changes as we shall demonstrate below. The recombination processes as well as spectral diffusion essentially occur on a time scale longer than 1 ns.

The PL decay over a longer time scale (ns - μs) has been measured with photon counting technique over the entire spectral range covered by the PL emission. The results are shown in Figure 8 and Figure 9 for selected samples at low temperature. In Figure 8 we compare the

time resolved spectra of an undoped (a) and a Si-doped sample (b) ($n = 2 \times 10^{18} \text{ cm}^{-3}$), respectively. The two spectra show a similar behavior as the stationary spectra in Figure 6 concerning the upshift with Si-doping. It is noted that the spectra for the doped samples are considerably narrower, with the impression that the lower energy part of the spectrum in Figure 8 (a) is simply missing in the spectrum (b). This will be discussed further below. There is also a rather strong shift downwards for the peak energy with delay time, which is expected due to screening by the excited e-h pairs, and also due to spectral diffusion by carrier hopping before recombination.

In Figure 9 we show a few examples of decay curves for various photon energies across the emission. Clearly the decay curves are very nonexponential, with a clear tendency towards a faster decay at the higher photon energy end of the emission. At long decay times (Figure 9 (b)), there is virtually no difference in the decay behavior for different parts of the emission, however.

In Figure 10 we show a comparison of the time-resolved spectra taken at 2 K and 300 K, for an MQW sample with the InGaN layers grown at 700 °C. The spectra show a quite similar downward shift with delay time, but the 300 K spectrum is broadened considerably and selectively on the high energy side, even at long delay times. This will be discussed below in connection with the strong localization potentials in the system. Also, the decay is faster at 300 K, presumably due to the presence of a nonradiative recombination component at this temperature. The low temperature decay times are identified as the radiative decay times in the MQWs, since they are independent of the excitation power.

The values of the decay times are not well-defined at any temperature, since the decay curves are not exponential. Defining an effective decay time (measured as the time for a decrease of intensity by a factor 1/e of the initial value) we obtain a value about 30 ns at 2 K for the sample with the InGaN layers grown at 700 °C and about 150 ns at 2 K for the sample with the InGaN layers grown at 780 C (both samples were undoped). The effective decay times for these two samples are illustrated at three different temperatures in Figure 11 (a, b). The temperature dependence of the decay times is not strong; in fact it seems like the radiative decay times are rather independent of temperature, so that the faster decay at 300 K is due to the presence of a nonradiative component at this temperature. Our measurements do not allow an accurate separation of radiative and nonradiative decay times at room temperature, however. Also, the sample in Figure 11 (a), with InGaN growth temperature 700 °C, evidently has a shorter radiative decay time. This might be related to some unknown difference

in the short range structure of the alloy in the QW with different InGaN growth temperature.

4 Discussion

4.1 The expected influence of the PZ field on PL spectra

In several papers on PL spectra and recombination for InGaN MQWs the PL spectrum consisted of more than one peak [2] [11] [12]. Several explanations have been offered for such multi-peak spectra, the most frequent being related to the segregation problem in the InGaN, i.e. the different peaks are due to regions with different In composition in the InGaN QW material. Our data do not show such behavior, i.e. only a single PL peak is observed.

The shape of the broad PL spectrum from these InGaN MQWs does not give any direct hint towards the recombination mechanism. The somewhat narrower PL peaks observed in similar systems with lower In composition can more consistently be ascribed to QW excitons [2] [5] [13]. For the broader peaks observed in this case, it is not obvious that excitons are involved. Further, the relative importance of the PZ field effects vs localization in potential fluctuations for the PL lineshape has to be determined. We shall below attempt to develop a coherent picture of the recombination process in these MQW systems, considering the total experimental information developed above.

In order to compare our results with previous data published in literature we need to point out that the description of the relation between composition x and bandgap of $\text{In}_x\text{Ga}_{1-x}\text{N}$ is quite confusing in the literature. Recent data suggest a rather high value for the bowing parameter (in the range 2.6 – 3.8 eV) for pseudomorphically strained InGaN layers for x -values $x = 0$ to $x = 0.25$ [9] [14] [15], while other data suggest a bowing parameter in this case of only about 1 [1] [2] [13]. In this work the higher bowing parameter has been used [9]. This means that when comparing with our data the x -values given in many earlier papers need to be reduced by a factor approximately 2, in order to allow a proper comparison of the optical data.

The following relation of the bandgap of a pseudomorphically strained $\text{In}_x\text{Ga}_{1-x}\text{N}$ layer vs x has been adopted in this work:

$$E_g(x) = 3.50(1-x) + 1.97x - 2.6x(1-x) \text{ eV}$$

at 2 K. This expression is the same as given in Ref [14], but up-shifted in energy by 0.08 eV to compensate for the bandgap increase between 300 K and 2 K. For $x = 0.15$ we then obtain $E_g = 2.94$ eV at 2 K. This value is consistent with the PL peak positions in Figure 3, con-

sidering a Stokes shift of about 100 meV. Assuming that 75 % of the band offset is in the conduction band [16], an electron effective mass of $0.22 m_0$, a hole effective mass of $1.0 m_0$ [17], we have solved the transcendental textbook equations [18] for the confinement energies in the QW. These energies for electrons and holes add to about 0.11 eV, leading to an estimated QW bandgap of about 3.05 eV at 2 K for $x = 0.15$ and a QW width of 30 Å.

The energy position of the broad PL peak is consistent with a downshift expected from a strong piezoelectric field across the QW, as first described by Takeuchi et al. [4]. The peak position observed for undoped MQW samples in low intensity stationary PL spectra (about 2.65 eV), as well as in the timeresolved spectra at a long time delay after the excitation pulse, are in good agreement with the spectral positions projected in Ref. [4] for MQW samples with similar In compositions. The downshift from the estimated unperturbed QW bandgap energy is about 0.4 eV. We therefore conclude that the PL peak position is consistent with a major effect of the PZ field across the QW. The value of the PZ field necessary to explain the large downshift is about 1 MV/cm, in agreement with previous work [4] [5]. (Since the spontaneous polarization (SP) effect is believed to be an order of magnitude smaller in this InGaN QW system, as compared to the PZ polarization, the SP induced fields are neglected in our discussion in this paper). As discussed further below, potential fluctuations are indeed the origin of part of this shift, however.

4.2 Screening effects by donors and carriers

The rather large upward shifts of the PL peak position with Si donor doping in the QWs, as well as with excitation intensity, points towards strong effects of carrier screening of the piezoelectric field as well as of the potential fluctuations. We have made an investigation of the effect of donor screening on the PZ field. The most extreme screening effect one could achieve from shallow donors would be if one puts all the donor ions on one side and the electrons on the other side of the QW; this would be a gross overestimation of the ability of the carriers to screen the field. We found with this approximation that this screening would only reduce the potential drop across the well with 12%, for the highest doping concentration $2 \times 10^{18} \text{ cm}^{-3}$. A similar modelling with ordered electron-hole pairs at this density, as required to simulate the spectral shifts with excitation intensity and delay time, gives the same result. A doping (or excited electron-hole pair) concentration of the order 10^{19} cm^{-3} would be needed to reproduce the observed maximum experimental shifts described above (see also Ref. [19]). We conclude that a perfect QW system affected essentially by the PZ field is not a proper model

for the observed behaviour of this MQW system. Obviously it needs a rather drastic modification, which is supplied by the potential fluctuations in the QWs.

From the magnitude of the Stokes shift in Figure 5 (a,b) and from the PL line widths there is evidence for the presence of potential fluctuations of the order at least 0.1 eV in the QWs. We have made some simple modelling to find out if the doping induced blue shift of the PL spectrum (Figure 6) could be reproduced from lateral screening of potential fluctuations in the QW. In a 3D system we know that the screening increases with carrier concentration; the Thomas-Fermi screening length decreases. In a 2D system the Thomas-Fermi screening length is unaffected by a change in carrier concentration. However, the Thomas-Fermi screening length only describes the screening of a slowly varying potential or the resulting potential far away from the center of the potential. The higher the carrier concentration is, the better the system screens a rapidly varying potential or the core of the potential. This means that the effective depth of a potential well caused by fluctuations can vary with doping or carrier concentration. In the present discussion we assume that the shallow donor electrons are ionized, e. g. by the strongly fluctuating electric field in the QW.

The behaviour of the 2D, low temperature, RPA dielectric function was shown in figure 4 (a) of Ref. [20] for different electron concentrations. The analytical expression for the dielectric function is:

$$\epsilon(\mathbf{q}, 0) = \begin{cases} 1 + \frac{2me^2}{\hbar^2 \kappa q} ; q \leq 2k_F \\ 1 + \frac{2me^2}{\hbar^2 \kappa q} \left(1 - \sqrt{1 - (2k_F/q)^2} \right) ; q > 2k_F \end{cases}$$

It was first derived by Stern [21]. We have modelled a potential of the form $V(r) = V(0)e^{-\beta^2 r^2}$, i.e., a Gaussian potential. (Figure 12 (a)). We chose the parameter β to be 0.01 \AA^{-1} , which means that the potential has a spatial extent of 100 \AA . The resulting curves in Figure 12 (a) scale with the strength of the potential, and therefore the plot in Figure 12 (a) is normalised. If we choose the unscreened value $V_0(0) = 390 \text{ meV}$ (i. e. the value expected in the absence of screening electrons) we get the well depths equal to 272 meV, 234 meV and 134 meV, respectively for the densities $2 \times 10^{17} \text{ cm}^{-3}$, $4 \times 10^{17} \text{ cm}^{-3}$ and $2 \times 10^{18} \text{ cm}^{-3}$. This corresponds to the blue shifts 38 meV and 100 meV as compared to the experimental values 40 meV and up to 200 meV, respectively,

when going from $2 \times 10^{17} \text{ cm}^{-3}$ to $4 \times 10^{17} \text{ cm}^{-3}$ and from $4 \times 10^{17} \text{ cm}^{-3}$ to $2 \times 10^{18} \text{ cm}^{-3}$.

In Figure 12 (b) we show the results of a calculation of the dependence of this short range 2D screening on the extent of the Gaussian potential. This is of interest, since in our samples we have no direct experimental information on the extension of the short range perturbation potentials. It is clear from Figure 12 (b), that the screening efficiency varies most strongly with electron density for potentials of an extent $50 - 150 \text{ \AA}$.

In order to explain the large spectral shifts observed with doping we therefore need to assume that the presence of rather strong potential fluctuations $V_0(r)$ in the QW over a short distance of 100 \AA . The unscreened magnitude of these fluctuations could be as large as 0.4 eV. The partly screened potentials seen in the experiment may be considerably weaker, however.

A major effect not taken into account in the simple screening model above is carrier transfer, which needs to be considered in a realistic model to explain the experimental data. In the above discussion the average electron concentration from the donors was considered. In practice, assuming the presence of rather short range potential fluctuations, carrier transfer processes (hopping) between different potentials may easily occur before recombination. The carriers will then have a tendency to be transferred to the lowest energy fluctuating potentials, selectively screening these. This transfer effect would explain part of the upshift of the PL peak with doping (Figure 6), and the apparent absence of the low energy part of the PL spectrum in the timeresolved spectra in Figure 8 (b). The size of the typical bare fluctuation potential $V_0(r)$ needed to explain the spectral shifts is therefore smaller than the one estimated above, but would still realistically be of the order 0.2 – 0.3 eV in our samples. Considering a typical background doping of about $2 \times 10^{17} \text{ cm}^{-3}$, the average depth of the experimentally observed screened potentials $V(r)$ should be of the order 0.1 – 0.2 eV to explain our data.

A spectral downshift with delay time observed in the timeresolved PL spectra is expected to occur, due to screening of the PZ field by the photoexcited carriers. Excited electron - hole pairs (or excitons) will be polarized in the PZ field in the QW and are thus expected to screen the PZ field quite efficiently. Total screening is expected at a very high e-h density, of the order 10^{19} cm^{-3} , in this case, as discussed above [20]. This is also reasonably consistent with the data recently published for modulation-doped InGaN MQW samples [22]. However, considering again the presence of strong potential fluctuations and lateral screening of these, a much lower carrier concentration may cause substantial

spectral shifts. At short delay time (say < 1 ns) after the pulse the PL peak position is at about 2.9 eV (Figure 10 (a)). The difference between this value and the unperturbed QW bandgap 3.05 eV is 0.15 eV, and should be made up from both the residual PZ field-induced Stark shift and the Stokes shift from the localization in the partially screened potential fluctuations, both probably of comparable magnitude. The maximum observed downshift with delay time in some cases is larger than 200 meV for the time-delayed spectra observed with short pulse excitation (Figure 10 (a)). This requires an initial excited excess carrier density of the order a few 10^{18} cm^{-3} , which is realistic under our experimental conditions. Most of the shift occurs during the first 10 ns, as expected in the screening model since the decay is fastest during this period. We note, however, that this spectral downshift with delay time should be composed of two contributions: the PZ induced Stark shift which is enhanced by a reduced screening at longer delay times, and the recombination of carriers from localization potentials, which become progressively deeper as the screening carrier concentration declines upon decay of the PL emission. It is difficult without a detailed modeling to judge which of these processes dominates, we only conclude here that they appear to be of comparable magnitude in our samples. As further discussed below, the potential fluctuations are in these QWs enhanced by the action of the PZ field. Therefore shifts due to these two effects are indeed closely connected.

4.3 Origin of potential fluctuations.

Having concluded that potential fluctuations are important in this MQW system, we need to discuss their possible origin. One obvious cause is the alloy fluctuations, which are always present in any alloy, but of different size due to the relative difference in the atomic pseudopotentials [23] [24] [25]. In the InGaN system these fluctuations are expected to be enhanced by segregation effects [7] [8], in particular if the growth of the InGaN layers takes place at a temperature above 750 °C. Another source of fluctuations that is wellknown for QW systems is due to the interface roughness. There is a dispersion in the QW bandgap value with QW width, which naturally is translated into a distribution of QW bandgap energies if the interfaces are rough. The observation of these effects of interface roughness in optical spectra depends on the length scale of these fluctuations. If this length scale is less than the extent of the exciton wavefunction, the effects will be averaged in optical spectra, and a broadening will be observed of the resulting PL spectra, as discussed in detail for the AlGaAs/GaAs QW system [26] [27].

In the present case with InGaN QWs these fluctuations will be enhanced by the presence of local strain.

Both fluctuations in In composition and QW width directly translate into a corresponding fluctuation in the size of the local strain field, since the InGaN layers are coherently grown on a thick GaN layer. The strain fluctuation itself will change the bandgap locally, this effect will be enhanced by the effect of the PZ field, which is also directly proportional to the in-plane strain [4] [28]. The combined action of these effects explains the rather strong potential fluctuations observed in this system, probably of the order 0.2 eV for this particular In composition, under our growth conditions. The width of the PL emission is clearly a measure of the size of these potential fluctuations. In order to get a precise relation between linewidth and the average depth of potential fluctuations a more detailed modeling is needed, to establish e.g. which potential depth is most active in a particular time window during decay of the PL emission. Such modeling is not warranted without independent data for the localization potentials.

4.4 The detailed recombination process. Excitons or free carriers?

Clearly excitons have a rather large binding energy in the InGaN QWs and are therefore as such thermally stable particles well above room temperature. An important question is whether excitons will survive in the QW in the presence of strong potential fluctuations. Such fluctuations are necessarily connected with corresponding lateral electric field fluctuations in the plane of the QW. In the presence of carriers the threshold field for impact excitation is rather small. In bulk GaN it has been shown to be of the order 10 V/cm [29], no corresponding experiments have been performed in GaN/InGaN QWs. We may assume that the threshold field for impact ionization in the QW is about an order of magnitude higher than for bulk GaN, in analogy with the situation in GaAs/AlGaAs QWs [30]. A fluctuating field of the order 100 V/cm in the QW plane would thus be sufficient for impact excitation of excitons, provided energetic carriers are present in the initial relaxation process. In reality these fluctuating fields are much larger, of the order $10^3 - 10^5$ V/cm, depending on the lateral extent of the short range localization potentials [31]. Already a random distribution of donors at a total residual density of 10^{17} cm^{-3} is sufficient to cause local fields of the order kV/cm in the QW plane. In fact the fluctuations modeled in Figure 12 invoke a lateral field of the order 10^6 V/cm at the short range potential fluctuations. We may therefore assume that the excitons initially created by optical excitation in the QW are ionized to a large extent via the interaction with energetic carriers (electrons) which are present during the initial relaxation process.

Another argument for the dominance of free carriers in the recombination process is derived from the observed radiative decay times. For an excitonic process in a 30 Å QW the PZ field has been estimated to reduce the oscillator strength by about a factor 3 compared to the case of no PZ field [32]. Assuming an excitonic radiative lifetime (localized QW excitons) of < 1 ns at 2 K, the exciton decay time would not be more than 3 ns. Our observed values are of the order 100 ns, i.e. more than one order of magnitude larger, as expected if recombination between free (or separately localized) carriers dominates. It should be pointed out that in QWs with considerably smaller In composition, and consequently smaller potential fluctuations, the recombination appears to be dominated by excitons [4] [5]. Also, the PL linewidth is then smaller than reported in this work [4] [5].

If we assume that most of the recombination in our samples actually occurs with separately localized electrons and holes, this will have consequences for the detailed interpretation of the spectral linewidth. Clearly if electrons and holes localize independently and diffuse via an acoustic phonon assisted hopping process [33], they will be able to lower the recombination photon energy more than in the case of excitons. The width of the PL peak could therefore partly be explained as recombination of localized electron-hole pairs, with a variation in e-h distance, also giving a spread in radiative lifetimes. These processes (i.e. a varying e-h distance and the hopping) are also consistent with the nonexponential decay behavior observed, as well as the spectral diffusion during the decay (in fact in a similar way as with the screening of the PZ field) [34]. As mentioned before, potential fluctuations of the order 0.1 - 0.2 eV may easily exist, sufficient to explain the emission peak shape. In addition, part of the line width might be explained by some minor fluctuations in the properties between the five QWs building up the structure.

As mentioned above, the radiative lifetime appears to be approximately independent of temperature up to room temperature. This is a typical behavior for recombination of localized carriers (or excitons for that matter), independent of the dimensionality of the system. Fluctuations of the order > 0.1 eV might cause localization up to the room temperature region. A temperature independent radiative lifetime is therefore not an exclusive argument for the presence of "quantum dot excitons" in the system [2]. A definite proof of the QD exciton model would be the observation of very sharp exciton lines in near field micro-PL experiments, which was so far not reported [35] [36]. It is likely that QD excitons do exist, but the topology of the localization potentials may be complicated, and further the QD exci-

ton recombination may be largely obscured by other processes, such as e.g. separate carrier recombination.

Finally we would like to comment on the shape of the PLE curves as shown in Figure 5. The curve has the shape of a continuous ramp with no obvious excitonic features. Clearly the ground state exciton would have a very low oscillator strength in a strong PZ field, and is not expected to be seen. Excited excitonic states could be expected, but in our case the electrons are probably not confined in the QW, they are pushed up above the conduction band of the barrier. The potential fluctuations may broaden and wipe out any peaks to be expected in the absorption of excited excitonic states. In addition the lifetimes of such excited states are expected to be very short, also a source of spectral broadening. Clearly the above discussed impact processes will also contribute to a broadening of the excitonic absorption shapes in this case. The combination of these effects will wipe out the otherwise expected excitonic absorption edge in this case.

5 Summary and conclusions

We conclude that in our $\text{In}_{0.15}\text{Ga}_{0.85}\text{N}/\text{GaN}$ multi quantum well structures the spectral position of the broad PL peak is predominantly determined by the piezoelectric field caused by the coherent strain in the quantum wells. We argue that the recombination is largely caused by separately localized electrons and holes, in the QW potential which is severely distorted by the PZ field. Strong potential fluctuations (of the order 0.1-0.2 eV) determine the width of the peak. These fluctuations are enhanced by the presence of the PZ field, but weakened by lateral electron screening. Such a two-dimensional electron screening of the potential fluctuations is an important process in donor-doped structures as well as at high excitation intensities.

Comparing with previous results in literature there is still a rather scattered picture concerning the recombination processes in this important QW system. It seems probable that different authors indeed have used samples which are rather different. One confusion is that a different scale for determining the In composition was used in different works; in many earlier papers the In composition should be regarded as a factor 2 smaller than reported, to allow a meaningful comparison with the data in this work. With this fact in mind it still seems clear that it is possible to grow InGaN QW material so that the composition fluctuations are quite large (by a higher temperature for the InGaN layer growth), while the PZ field can be screened to a large extent by Si-doping [11]. In that way the fluctuations may sometimes be the dominant factor governing the recombination processes, as claimed in some previous work [11]. In our case, however, the PZ field appears to have a strong

effect on the QW potential and also influencing the recombination processes in the QWs. Strong potential fluctuations are clearly present, however, and cause the carriers to be essentially localized up to room temperature in an undoped QW at moderate excitation intensities. Therefore we conclude that lowering the growth temperature of the InGaN layers down to as low as 700 °C does seem to remove the short range potential fluctuations related to In segregation.

ACKNOWLEDGMENTS

The work at Meijo was supported in part by the Japan Society for the Promotion of Science Research for the Future Program in the Area of Atomic Scale Surface and Interface Dynamics under the project of "Dynamical Process and Control of the Buffer Layer at the Interface in a Highly-Mismatched System (JSPS96P00204)", the Ministry of Education, Science, Sports and Culture of Japan, (High-Tech Research Center Project and contract number 11450131) and the Murata Science Foundation.

REFERENCES

- [1] Shuji Nakamura, Gerhard Fasol, *The Blue Laser Diode - GaN based Light Emitters and Lasers*, (Springer-Verlag, Heidelberg, 1997), .
- [2] Y. Narukawa, Y. Kawakami, S. Fujita, S. Fujita, S. Nakamura, *Phys. Rev. B* **55**, R1938 (1997).
- [3] Y. Narukawa, Y. Kawakami, S. Fujita, S. Nakamura, *Phys. Rev. B* **59**, 10283 (1999).
- [4] T. Takeuchi, S. Sota, M. Katsuragawa, M. Komori, H. Takeuchi, H. Amano, I. Akasaki, *Jpn. J. Appl. Phys.* **36**, L382 (1997).
- [5] Andreas Hangleiter, Jin Seo Im, H. Kollmer, S. Heppel, J. Off, Ferdinand Scholz, *MRS Internet J. Nitride Semicond. Res.* **3**, 15 (1998).
- [6] I Akasaki, H Amano, *Jpn. J. Appl. Phys.* **36**, 5393 (1997).
- [7] A. Koukitu, N. Takahashi, T. Taki, H. Seki, *J. Cryst. Growth* **170**, 206 (1997).
- [8] T. Saito, Y. Arakawa, *Phys. Rev. B* **60**, 1701 (1999).
- [9] C Wetzell, T Takeuchi, S Yamaguchi, H Katoh, H Amano, I Akasaki, *Appl. Phys. Lett.* **73**, 1994-6 (1998).
- [10] Y. Kawaguchi, M. Shimizu, K. Hiramatsu, N. Sawaki, *Mater. Res. Soc. Symp. Proc.* **449**, 89 (1997).
- [11] T. Deguchi, A. Shikanai, K. Torii, T. Sota, S. Chichibu, S. Nakamura, *Appl. Phys. Lett.* **72**, 3329 (1998).
- [12] P. Perlin, C. Kisielowski, V. Iota, B. Weinstein, L. Mattos, N.A. Shapiro, J. Kruger, E.R. Weber, J. Yang, *Appl. Phys. Lett.* **73**, 2778-2780 (1998).
- [13] K. C. Zeng, M. Smith, J. Y. Lin, H. X. Jiang, *Appl. Phys. Lett.* **73**, 1724 (1998).
- [14] T Takeuchi, H Takeuchi, S Sota, H Sakai, H Amano, I Akasaki, *Jpn. J. Appl. Phys.* **36**, L177 (1997).
- [15] M. D. McCluskey, C. G. Van de Walle, C. P. Master, L. T. Romano, N. M. Johnson, *Appl. Phys. Lett.* **72**, 2725 (1998).
- [16] CG Van der Walle, J Neugebauer, *Appl. Phys. Lett.* **70**, 2577-2579 (1997).
- [17] M. Suzuki and T. Uenoyama, in "Group III Nitride Semiconductot Compounds, Physics and Application" edited by B. Gil, Oxford University Press 1998, pp 307
- [18] G. Bastard, *Wave Mechanics Applied to Semiconductor Heterostructures*, Les Edition de Physique, Paris, 1982
- [19] F. Della Sala, A. Di Carlo, P. Lugli, F. Bernardino, V. Fiorentini, R. Scholz, J. -M. Jancu, *Appl. Phys. Lett.* **74**, 2002 (1999).
- [20] B. Monemar, J.P. Bergman, J. Dalfors, G. Pozina, B.E. Sernelius, P.O. Holtz, H. Amano, I. Akasaki, *MRS Internet J. Nitride Semicond. Res.* **4S1**, G2.5 (1999).
- [21] F. Stern, *Phys. Rev. Lett.* **18**, 546 (1967).
- [22] Y. H. Cho, J. J. Song, S. Keller, M. S. Minsky, E. Hu, U. K. Mishra, S. P. DenBaars, *Appl. Phys. Lett.* **73**, 1128 (1998).
- [23] E. F. Schubert, E. O. Göbel, Y. Horikoshi, K. Ploog, H. J. Quiesser, *Phys. Rev. B* **30**, 813 (1984).
- [24] R. Zimmermann, *J. Cryst. Growth* **101**, 346 (1990).
- [25] S. M. Lee, K. K. Bajaj, *J. Appl. Phys.* **73**, 1788 (1993).
- [26] C. Weisbuch, R. Dingle, A. C. Gossard, W. Wiegmann, *Sol. St. Comm.* **38**, 709 (1981).
- [27] G. Bastard, C. Delalande, M. H. Meynadier, P. M. Frijlink, M. Voos, *Phys. Rev. B* **29**, 7042 (1984).
- [28] C. Bodin, R. André, J. Cibert, Le Si Dang, D. Bellet, G. Feuillet, P. H. Jouneau, *Phys. Rev. B* **51**, 13181 (1995).
- [29] D Volm, K Oettinger, T Streibl, D Kovalev, M Ben-Chorin, J Diener, BK Meyer, J Majewski, L Eckey, A Hoffman, H Amano, I Akasaki, K Hiramatsu, T Detchprohm, *Phys. Rev. B* **53**, 16543-16550 (1996).
- [30] H. Weman, G. M. Treacy, H. P. Hjalmarsson, K. K. Law, J. L. Merz, A. C. Gossard, *Phys. Rev. B* **45**, 6263 (1992).
- [31] A. V. Buyanov, J. P. Bergman, J. A. Sandberg, B. E. Sernelius, P. O. Holtz, B. Monemar, H. Amano, I. Akasaki, *Phys. Rev. B* **58**, 1442 (1998).
- [32] Marco Buongiorno Nardelli, Krzysztof Rapcewicz, J. Bernholc, *Appl. Phys. Lett.* **71**, 3135 (1997).
- [33] T. Holstein, S. K. Lyo, R. Orbach, "Excitation transfer in disordered systems", in *Laser Spectroscopy of Solids*, edited by W. M. Yen and P. M. Selzer, Topics in Applied Physics, Vol. 49 (Springer Verlag, Berlin, 1981), p. 39.
- [34] I. Kuskovsky, G. F. Neumark, V. N. Bondarev, P. V. Pikhitsa, *Phys. Rev. Lett.* **80**, 2413 (1998).
- [35] P. A. Crowell, D. K. Young, S. Keller, E. L. Hu, D. D. Awschalom, *Appl. Phys. Lett.* **72**, 927 (1998).
- [36] A. Vertikov, M. Kuball, A. V. Nurmikko, Y. Chen, S. Y. Wang, *Appl. Phys. Lett.* **72**, 2645 (1998).

FIGURES

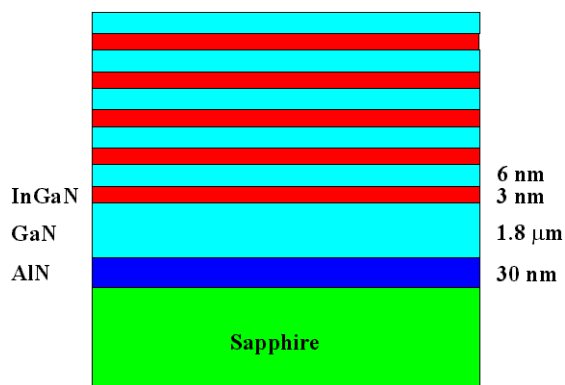


Figure 1. Schematic picture of the multiple quantum well sample structure used for this work.

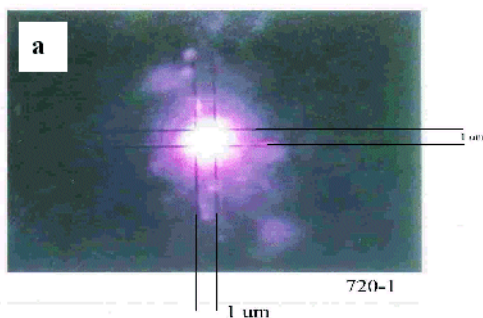


Figure 2a. Photoluminescence topograph at 300 K of the total emission from an InGaN/GaN MQW sample with the InGaN growth temperature 700 °C. Note that the laser spot has a Gaussian intensity profile. Intensity fluctuations on a length scale of a few μm are observed.

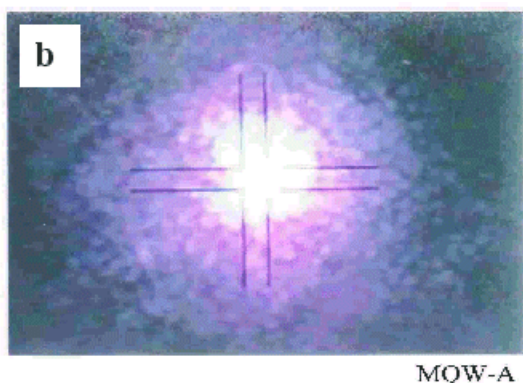


Figure 2b. The same type of data at 300 K for an InGaN/GaN MQW sample with the InGaN growth temperature at 780 °C. The length scale of intensity fluctuations is now smaller, but still resolved

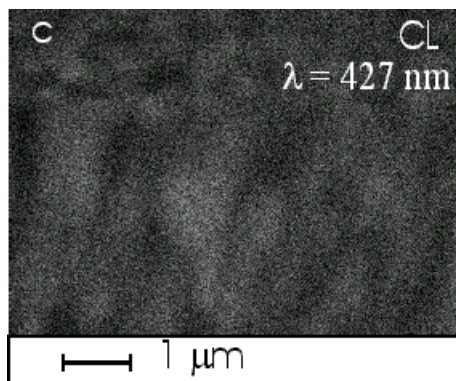


Figure 2c. Monochromatic cathodoluminescence topograph at 6 K from an InGaN/GaN MQW sample with the InGaN growth temperature at 700 °C. Again intensity fluctuations over a length scale of about 1 μm are observed.

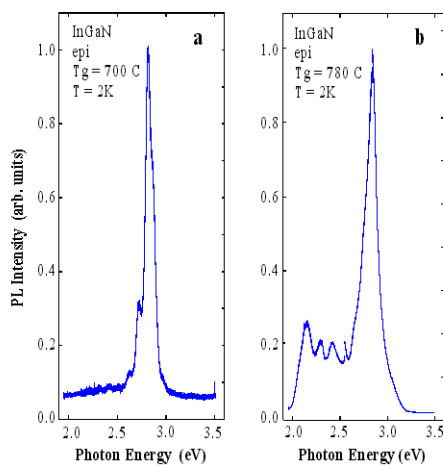


Figure 3. Stationary PL spectra at 2 K of two coherently strained thick $\text{In}_{0.15}\text{Ga}_{0.85}\text{N}$ epilayers grown on sapphire at the temperatures indicated: (a) left panel, 700 °C, (0.06 μm thick layer) (b) right panel, 780 °C (0.10 μm thick layer). Note that the presence of a spectral contribution at lower photon energies in (b) indicates some segregation.

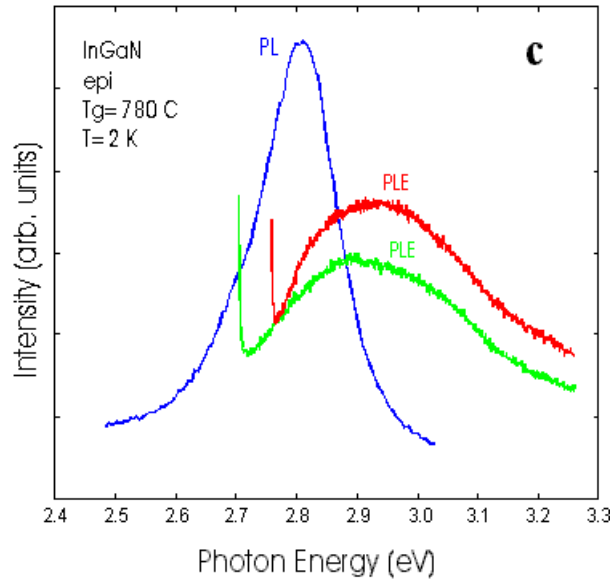


Figure 3c. In (c) are shown two PLE spectra for the same sample as in (b), detected at two different photon energies. The PL spectrum obtained with low intensity lamp excitation is also shown.

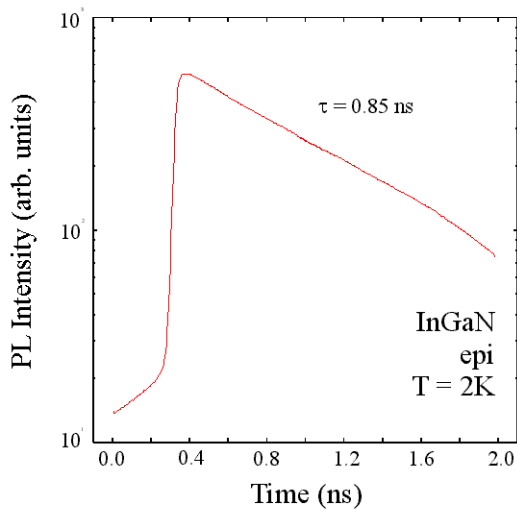


Figure 4. PL transient response at 2 K of the PL peak for the sample in Figure 3 (a). Note the welldefined radiative lifetime of 0.85 ns.

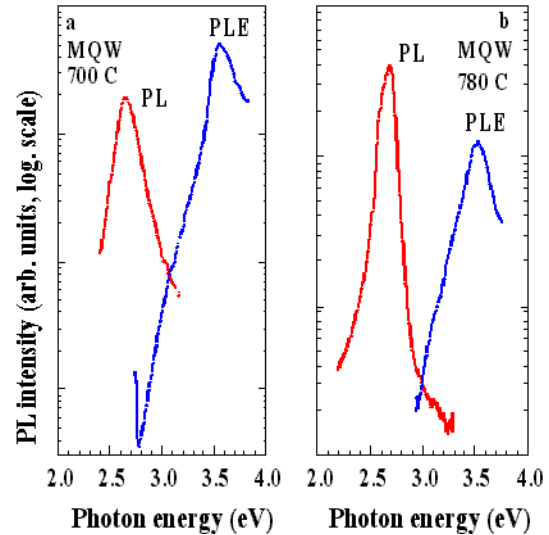


Figure 5. Stationary PL spectra as well as PLE spectra at 2 K of two coherently strained and nominally undoped $\text{In}_{0.15}\text{Ga}_{0.85}\text{N}/\text{GaN}$ MQWs grown on sapphire with the InGaN layer growth temperatures indicated: (a) left panel, 700 °C, (b) right panel, 780 °C. The spectra are obtained with low intensity excitation employing a Xe lamp. The PL signal at lower photon energies is very weak in both cases. The PLE spectra are obtained with detection at the peak of the PL signal.

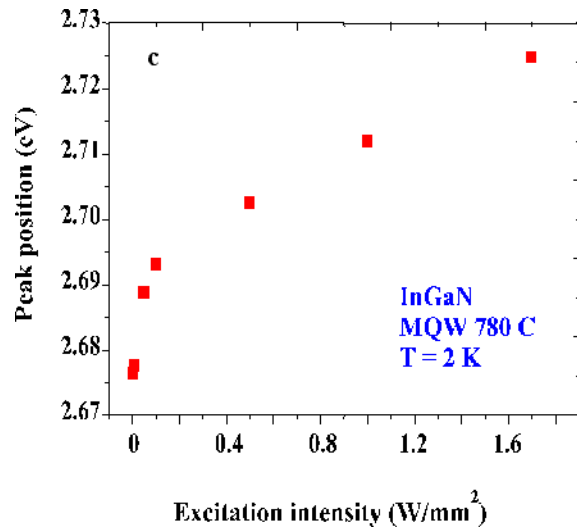


Figure 5c. In Fig 5 (c) is shown the dependence of the peak position on the excitation intensity for the same sample as in 5 (b).

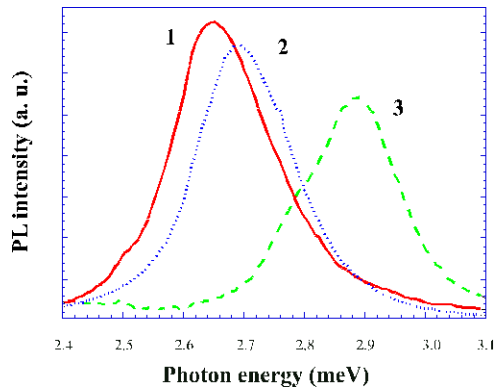


Figure 6. Stationary PL spectra at 2 K of three coherently strained $\text{In}_{0.15}\text{Ga}_{0.85}\text{N}/\text{GaN}$ MQWs grown on sapphire at 700 °C. Sample 1 is nominally undoped, but has a background Si donor doping of about $1 \times 10^{17} \text{ cm}^{-3}$ in the well. The other two samples are Si-doped in the wells, to a density of about $4 \times 10^{17} \text{ cm}^{-3}$ for sample 2 and about $2 \times 10^{18} \text{ cm}^{-3}$ for sample 3. The GaN barriers are not Si-doped.

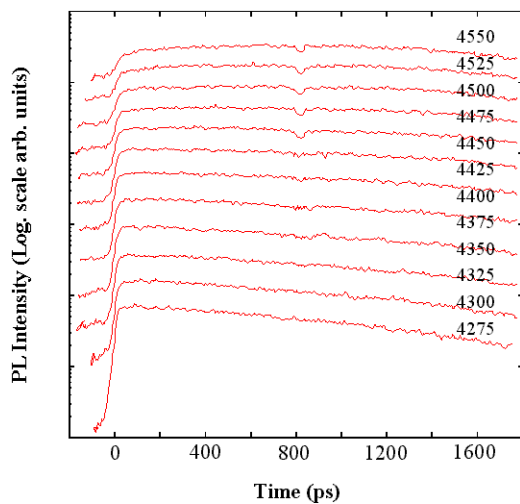


Figure 7. Streak camera panel at 2 K for the same MQW sample as in Figure 5 (a), obtained with fs pulse excitation at about 3.2 eV. Each transient is marked with the corresponding PL emission wavelength (in Å units). Note the short rise time across the whole broad PL spectrum.

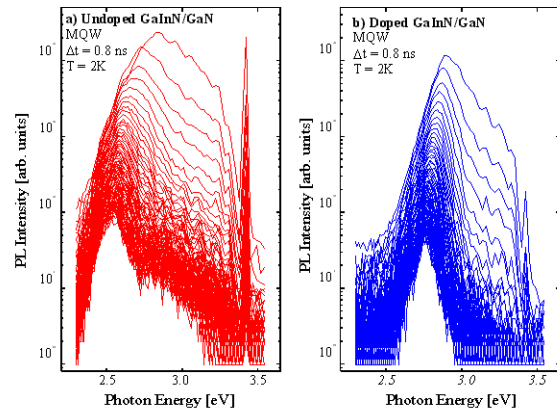


Figure 8. Timeresolved PL spectra for two MQW samples obtained at 2 K with excitation at 3.6 eV. The time interval between each spectrum is 0.8 ns. In (a) left panel, are shown spectra for the undoped sample D1 in Figure 6, and in (b) right panel, are shown corresponding data for the doped sample D3 in Figure 6. Note the strong spectral shift between the two samples.

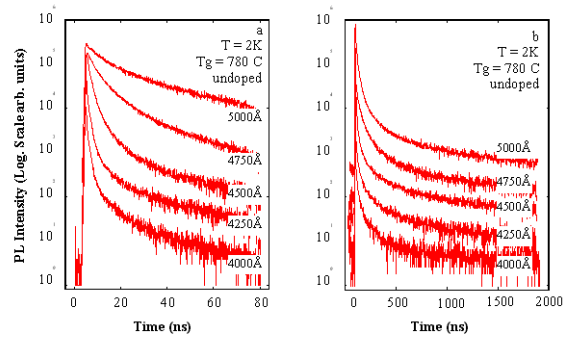


Figure 9. Decay curves at different photon energies within the broad PL peak, obtained at 2 K with excitation at 3.2 eV for the same MQW samples as in Figure 5 (b). In (a) left panel, is shown the intermediate time regime, on the right panel (b) is shown the long time behavior.

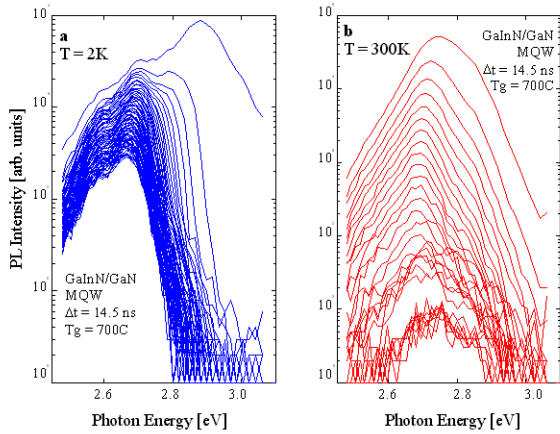


Figure 10. Timeresolved PL spectra for an MQW sample with the InGaN layer grown at 700 °C, obtained at 2 K, left panel (a) and at 300 K, right panel (b), respectively, and with excitation at 3.2 eV. The 300 K spectra are broadened towards higher energy, and also have shorter decay time.

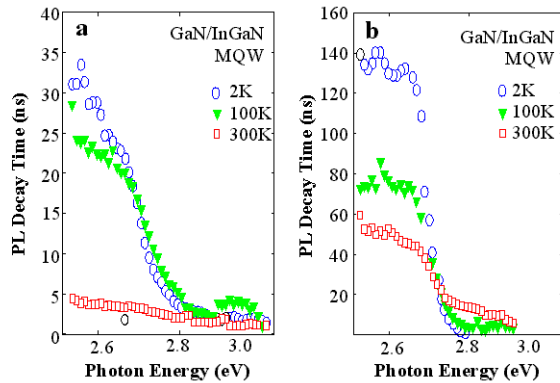


Figure 11. Effective decay times for the same two MQW samples as in Figure 5 (a), left panel, and (b), right panel, respectively. The data are shown for 3 different measurement temperatures, 2K, 100 K, and 300 K, and for a number of different wavelengths across the broad PL emission. The excitation wavelength is about 3.2 eV.

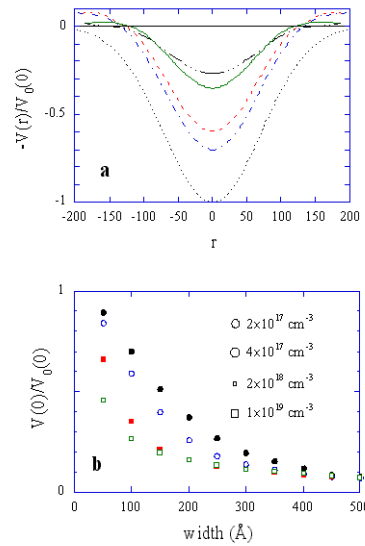


Figure 12. (a). The screening effect on a gaussian potential of width 100 Å in one of the quantum wells. The dotted curve is the bare potential. The dash-dotted, dashed, full and dash-triple-dotted curves are for the carrier concentrations $2 \times 10^{17} \text{ cm}^{-3}$, $4 \times 10^{17} \text{ cm}^{-3}$, $2 \times 10^{18} \text{ cm}^{-3}$ and $1 \times 10^{19} \text{ cm}^{-3}$, respectively. All curves have been scaled to the value at the center of the unscreened potential. We have plotted the potentials with reverted sign to get the impression of a potential well. The screened potentials have Friedel oscillations at large separations. (b). The well depths of screened gaussian potentials for different carrier concentrations, indicated in the figure, as functions of potential width.